

Monitoring and modelling spatio-temporal urban growth of Delhi using Cellular Automata and geoinformatics



Pratyush Tripathy^{a,b}, Amit Kumar^{a,*}

^a Department of Land Resource Management, Central University of Jharkhand, Ranchi 834205, India

^b Indian Institute for Human Settlements, Bengaluru 560080, India

ABSTRACT

The study encompasses spatio-temporal land use/ land cover (LULC) monitoring (1989–2014) and urban growth modelling (1994–2024) of Delhi, India to deduce the past and future urban growth paradigm and its influence on varied LULC classes integrating geospatial techniques and Cellular Automata (CA). The study focused on scrutinising the reliability of the CA algorithm to function independently for urban growth modelling, provided with strong model calibration. For this purpose, satellite data of six stages of time at equal intervals along with the population density, distance to CBD and roads, and terrain slope are used. The satellite-based LULC during 1989–2014 exhibited 457 km² of net urban growth (275% change), cloned by the simulated LULC with net increase 448 km² (270% change). The spatial variation analysis using the principal component analysis (PCA) technique exhibit high similarity in classification ranging from 72% to 88%. The statistical accuracy between the satellite-based and simulated built-up extent of 2014 resulted in the overall accuracy 95.62% of the confusion matrix, and the area under the receiver operating characteristic (ROC) curve as 0.928—indication high model accuracy. The projected LULC exhibit that the urban area will increase to 708 km² and 787 km², primarily in western and eastern parts during 2019 and 2014 respectively. The rapid urban growth will replace and transform others LULC (net loss 138 km²) followed by vegetation cover (net loss 26 km²) during 2014–24. This rapid urban growth is detrimental to the habitat and may trigger critical risks to urban geo-environment and ecosystem in Delhi. Therefore, the study necessitates towards decentralization of urban functions and restoration of varied LULC in order to regulate the future urban growth patterns for sustainable development. The GDAL and NumPy libraries in Python 3.4 were efficient in spatial modelling and statistical calculations.

1. Introduction

Hybrid models of CA (Cellular Automata) such as CA-MC (Markov Chain) models, CA-logistic regression (LR) models, and CA-MC-LR dominate existing geospatial and related literature (Arsanjani, Kainz, & Mousivand, 2011; Jokar Arsanjani, Helbich, Kainz, & Darvishi Boloorani, 2013; Mondal, Sharma, Garg, & Kappas, 2016; Munshi, Zuidgeest, Brussel, & van Maarseveen, 2014; Mustafa et al., 2018; Siddiqui et al., 2017); the identity of the CA model to produce convincing results autonomously has faded over time. This study analyses the spatio-temporal land use/land cover (LULC) dynamics in recent decades to model urban growth using the CA algorithm for Delhi, India. The paper scrutinises the ability of the CA algorithm to replicate real-world urban growth process and project future growth. Many researchers have affirmed the reliability of the CA model, but the focus on appropriate model calibration with equidistant temporal data remain scarce (Jat, Choudhary, & Saxena, 2017; Rafiee, Mahiny, Khorasani, Darvishsefat, & Danekar, 2009). For this purpose, the LULC for six different years—1989, 1994, 1999, 2004, 2009 & 2014—has been analysed in the present study.

In addition, the LULC data along with other growth driving

parameters such as proximity to roads and CBD (central business district), topography, population statistics, areas with growth restrictions, etc. were considered to project built-up extent for forthcoming years. The future built-up projection was useful to extrapolate the imminent influence of rapid urbanisation in Delhi on the environment, which could aid in framing sustainable measures. The study also reports the accuracy and reliability of the CA algorithm in modelling urban growth.

Urbanisation is a global phenomenon, having varied rates and trends across geographical regions (Lal, Kumar, & Kumar, 2017). The physical and urban forms leading to unplanned and unsustainable patterns of urban growth characterises the growth of urban areas (Kumar & Pandey, 2017). The physical and morphological conditions, economic state, population growth, political situation, policies, and social behaviour varies across regions that makes the pattern of urban growth unpredictable (Thapa & Murayama, 2010). A majority of Indian cities witnessed dramatic growth, degrading the environment and the ecosystem on a large scale (Diksha & Kumar, 2017; Kumar & Pandey, 2016; McMichael, 2000; Peng, Chen, & Cheng, 1997). Modelling the urban growth is necessary for quantitative assessment of the growth patterns to bring down the future effects of urbanisation on the environment and aid in policymaking. Previous studies reported the

* Corresponding author.

E-mail addresses: pratyush@ihs.ac.in (P. Tripathy), amit.kumar@cuj.ac.in, amit.iirs@gmail.com (A. Kumar).

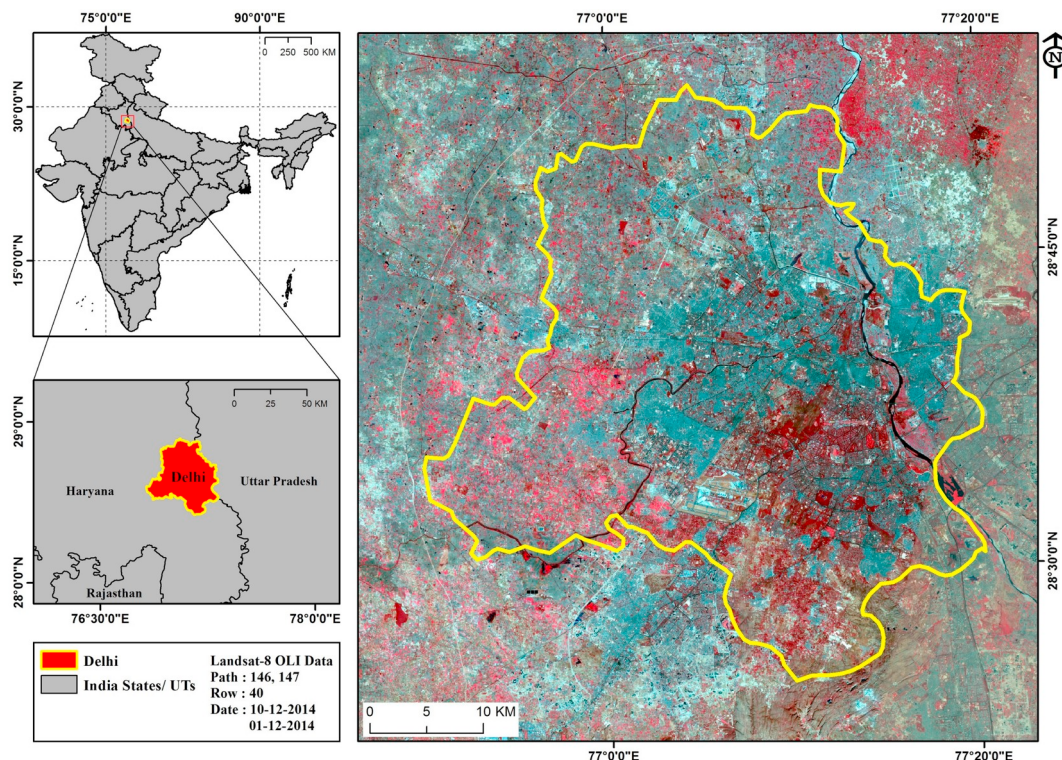


Fig. 1. Map of the study area (Delhi).

importance and necessity of performing a spatio-temporal analysis of urban growth in terms of locations, characteristics and consequences (Lo & Yang, n.d.; Aljoufie, Zuideest, Brussel, & van Maarseveen, 2013; Aljoufie, Zuideest, Brussel, van Vliet, & van Maarseveen, 2013; Clarke, Hoppen, & Gaydos, 1997; Dubovik, Sliuzas, & Flacke, 2011; Feng, Liu, Tong, Liu, & Deng, 2011; Jokar Arsanjani et al., 2013; Mitsova, Shuster, & Wang, 2011; Santé, García, Miranda, & Creciente, 2010; Thapa & Murayama, 2012).

Modelling urban growth using satellite data has become popular over time due to the scope of fusing statistical algorithms with remotely sensed data, availability of high-resolution satellite imagery, and increased computational power. Researchers have been analysing urban growth patterns and their driving factors using geospatial and statistical models, which include regression models (Hu & Lo, 2007; Nong & Du, 2011), CA (Berberoglu, Akin, & Clarke, 2016; Chen, Li, Liu, Ai, & Li, 2016; Deep & Saklani, 2014; Jat et al., 2017; Mustafa, Cools, Saadi, & Teller, 2017), Markov chain (Arsanjani et al., 2011), CA-Markov models (Jokar Arsanjani et al., 2013; Mondal et al., 2016) and CA-logistic regression models (Jokar Arsanjani et al., 2013; Mustafa et al., 2018). Among these established models, CA model is the most popular, as it is appropriate to simulate the process of urban growth, which is entirely local in nature (Clarke & Gaydos, 1998). The CA model is a rule-based approach working on a micro level in addition with flexibility of transition rules that simplifies spatial simulation (Torrens & O'Sullivan, 2001; Waldrop, 1992), therefore contributing to better projecting of urban growth as compared to conventional mathematical models (Batty & Xie, 1994). Different variants of CA models such as SLEUTH (Clarke et al., 1997), the dynamic urban evolution model (DUEM) (Batty, 1997), the multi-criteria evaluation (MCE)-CA model (Wu & Webster, 2000), the multi-agent system (MAS)-CA model (Ligtenberg, Bregt, & van Lammeren, 2001), the Voronoi-CA model (Shi & Pang, 2000) and the Markov-CA model (Vaz, De Noronha, & Nijkamp, 2014) have been developed to simulate urban land use change and urban expansion.

The transition rules for the CA modelling remains a point of major attention even after the achievements of CA in urban growth modelling (Batty, 1998). Accurate modelling using CA models requires convincing

transition rules and the highest possible calibration, which is a challenging task. Modelling and projection of urban growth using various thematic variables viz., land use/land cover, elevation, slope, proximity to transportation, distance to CBD, distance to large-sized cities, employment rate, richness index, zoning, hill shade, etc. was performed by various scholars (Berberoglu et al., 2016; Mustafa et al., 2018) for many large and medium cities in the world including Chicago, Washington-Baltimore area and San Francisco (Clarke & Gaydos, 1998), Tokyo (Zhao, Zhao, & Murayama, 2008), and Shanghai (Han, Hayashi, Cao, & Imura, 2009). Urban growth modelling within the Indian context has been reported previously for Mumbai (Shafizadeh Moghadam & Helbich, 2013), Kolkata (Bhatta, 2009), Bangalore (Ramachandra et al., 2013), Dehradun (Deep & Saklani, 2014) and Ahmedabad (Munshi et al., 2014). Such studies are of use in measuring the influence of rapid urbanisation on the environment and contribute to effective urban planning processes.

Delhi, India's capital, witnessed unprecedented urban growth and high population influx in the last few decades due to its multifarious functions, making it the second largest city after Mumbai in terms of population (Census, 2011). This growth steered into various urban, environmental and socio-economic problems viz., degradation of air quality, groundwater, surface water, green spaces (Guttikunda & Calori, 2013; Kumar, 2016; Li, Chen, Yan, & Yu, 2015; Maiti & Agrawal, 2005; Nagar et al., 2017; Ramachandraiah & Prasad, 2004; Sahu, Deori, & Ghosh, 2018; Sharma, Balyan, & Kumar, 2018). The urban area in Delhi has increased rapidly over the past few decades (Chadchan & Shankar, 2012; Jain et al., 2016; Mohan, Pathan, Narendrareddy, Kandya, & Pandey, 2011), therefore it seems necessary to analyse the trend of urban growth and deduce its future effects on other land cover features.

2. Study area

India's capital city - Delhi, covers 1483 km² of land and is located between 28.33° to 29.0° N latitude and 76.83° to 77.33° E longitude (Fig. 1). According to Census, 2011, Delhi's population is 11,034,555,

but the decadal growth has dwindled from 51.45% in 1981–91 to 47.02% in 1991–2001 to 11.2% in 2001–2011. The overall population density of Delhi has proliferated from 9,340 persons per km² in 2001 to 11,320 persons per km² in 2011, which is the highest among all other Indian states/UTs in India (*Statistical Abstract of Delhi*, 2014). From 2016 to 2030, Delhi is projected to outperform Mumbai in terms of growth, with GDP rising by 7.1% and 5.7% per year respectively (*Global Cities 2030*, 2016).

3. Methods and data used

This study deals with various thematic layers prepared using satellite imagery, Census of India data, and topographical sheets. Land use/land cover (LULC) maps were prepared using satellite datasets to understand the dynamics of urban growth from the year 1989 to 2014. Along with the LULC, various urban growth supporting factors viz., population density, slope, proximity to road networks and proximity to CBD (Central Business District) were prepared as raster layers for modelling purposes. In order to get the best possible threshold values, a model was calibrated carefully to keep the simulated LULC close to the actual LULC both statistically and spatially. The trend of the obtained threshold values was assessed for future built-up projections for the years 2019 and 2024. The LULC, road network and other thematic layers were prepared in ArcGIS ver. 10.3, whereas calibration and future projection were conducted in Python 3.4, using GDAL 2, Numpy 1.14, Matplotlib 2.2, and Scikit-Learn 0.19 libraries (Fig. 2).

3.1. Thematic layers

Multi-temporal LANDSAT satellite images acquired from the USGS website (<https://earthexplorer.usgs.gov>) for the years 1989, 1994, 1999, 2004, 2009 and 2014 were used to prepare LULC maps for the

said observation years using K-means classifier in four major classes viz., built-up, vegetation, and water bodies, among others. A brief description of used satellite data and major LULC classes are provided in Table 1 and Table 2.

The focus of the current study was to project the built-up feature class, which includes constructed areas such as residential areas, commercial complexes, institutions, and informal settlements. The land primarily under any type of green cover was classified as vegetation. The water bodies comprised rivers, ponds, canals, etc., and the remaining area was classified as others, which was primarily composed of wastelands, rock outcrops, agricultural fallow lands, etc. The satellite-based LULC-classified maps were validated using selective field checks (May 2017) as well as Google Earth images. The overall accuracy was calculated for each of the observation years (1989, 1994, 1999, 2004, 2009 & 2014), and it ranged from 89% to 95% whereas the kappa coefficient ranged from 0.85 to 0.93. The finalised LULC maps were used to analyse the land use/land cover change dynamics and urban growth during 1989–2014, and later to calibrate the model.

The zone-wise population density thematic layers were prepared using *United Nation Population Projection 2030* (2015) to calculate the population density for the years 2019 and 2024 using the unitary method. For previous years, Census of India population data (1991, 2001 and 2011) was considered for simulations falling in a particular decade. The population density maps for the years 1991, 2001 and 2011 were used during the model calibration process and, for future projection purposes, the years 2019 and 2024 population density maps were used. The densities were computed in the attribute of the vector layer of different zones of Delhi, later converted to raster layers of cell size 30 m × 30 m, so as to match the geometry of the other participating layers. The Cartosat – I Digital Elevation Model (DEM) of spatial resolution 30 m acquired from BHUVAN (<http://bhuvan.nrsc.gov.in>) was used to prepare slope maps in the three classes (< 3, 3–5, > 5).

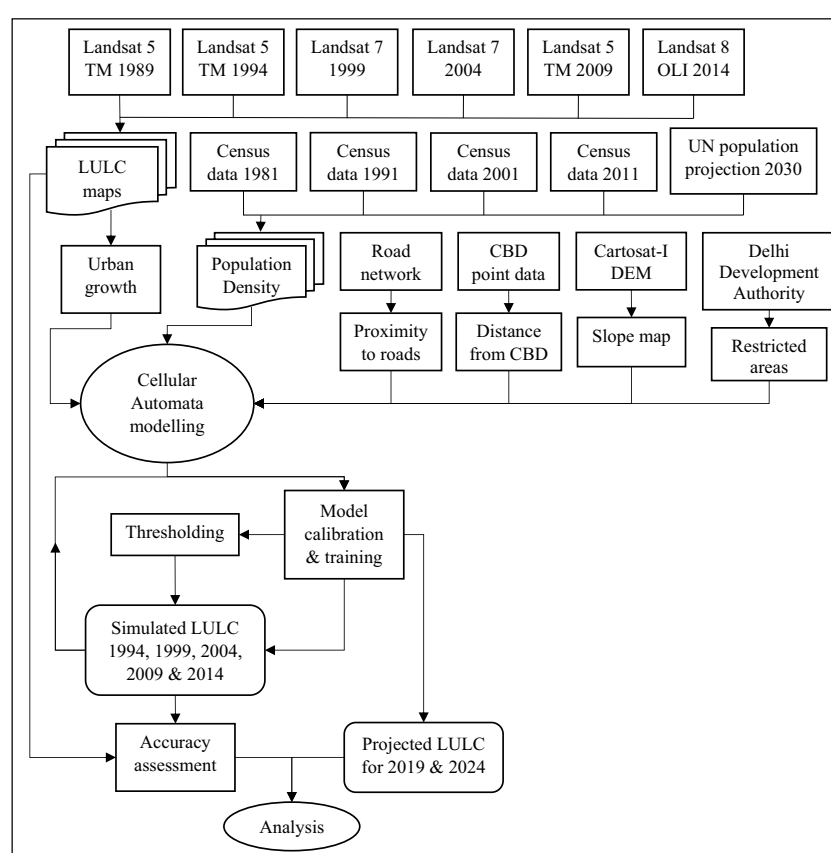


Fig. 2. Methods chart detailing the procedure adopted in the study.

Table 1
Details of input data used in the study.

Data type	Details	Date of acquisition
LANDSAT 5 TM	Path: 147, 146; Row: 40	1989/01/26, 1989/12/05
LANDSAT 5 TM	Path: 147, 146; Row: 40	1994/12/19, 1994/12/10
LANDSAT 7 ETM +	Path: 146, 147; Row: 40	1999/12/09, 1999/12/16
LANDSAT 7 ETM +	Path: 146, 147; Row: 40	2004/11/20, 2004/11/11
LANDSAT 5 TM	Path: 146, 147; Row: 40	2009/11/26, 2009/11/17
LANDSAT 8 OLI	Path: 146, 147; Row: 40	2014/12/10, 2014/12/01
Digital elevation model	Cartosat I-V3 (Spatial resolution - 30 m)	
Census of India		1991, 2001 and 2011
UN population division (2015)		2019 and 2024
Zone map of Delhi	Master Plan 2021	Delhi Metropolitan
DDA land use		

Table 2
Characteristics of LULC feature class.

Feature class	Characteristics	Description
Built-up	Consists of	All man-made structures that are primarily impervious including residential areas, commercial areas, mixed, with low to high economic relevance
	Proximity	Parks, plantations, lakes, ponds, transport networks
Vegetation	Significance	Very high to moderate population density
	Consists of	All green spaces within the urban area and its environs including agri-cropland, parks, plantations, protected forests, agriculture
Water	Proximity	Moderate to low built-up structures and water bodies
	Significance	Public, private and government preserved areas
Water	Consists of	All water bodies including surface water bodies, lakes, reservoirs, ponds, rivers
	Proximity	Low/high vegetation, open land, sandy areas, low built-up
Others	Significance	Potable/non-potable water, contaminated, irrigation
	Consists of	All features excluding built-up, vegetation, and water; including vacant/wasteland, fallow agricultural land, sandy areas, rock outcrops etc.
Others	Proximity	Low vegetation, low built-up structures
	Significance	Belonging to private or government agencies, individuals

The major road network obtained from topography sheet was reshaped using recent LANDSAT images (2014) to generate the raster representing proximity to major roads, classified at 500 m intervals up to 5 km, and 1000 m intervals beyond it. Similarly, multiple buffer rings around the CBD location (considering Connaught Place, Delhi) were taken at 5 km intervals in 10 classes. The vector layers were rasterised at 30 m cell size and clipped with a constant extent to match the geometry of the former layers.

To enhance the capability of the model in replicating the actual world growth process, a dichotomous layer for restricted and non-restricted areas was considered. This binary layer trained the model not to generate built-up pixels in restricted areas near to the central ridge reserve forest, commercial airport and certain urban locations.

3.2. CA model algorithm

The script for CA model was formulated to consider all the factors which contribute to urban growth in Delhi. A 3×3 size kernel held the test pixel at its center, as shown in Eq. (i).

$$A_{i,j}^t = \begin{bmatrix} a_{i-1,j-1}^{(t)} & a_{i-1,j}^{(t)} & a_{i-1,j+1}^{(t)} \\ a_{i,j-1}^{(t)} & a_{i,j}^{(t)} & a_{i,j+1}^{(t)} \\ a_{i+1,j-1}^{(t)} & a_{i+1,j}^{(t)} & a_{i+1,j+1}^{(t)} \end{bmatrix} \quad 3 \times 3 \text{ neighbourhood} \quad (i)$$

The model depends primarily on the current state of the test pixel, the current state of immediate neighboring pixels and the set of transition rules (Kumar, Mukhopadhyay, & Ramachandra, 2009). Matching the geometry of layers is crucial to ensure that any random pixel $a_{i,j}$ represents the same piece of land in all the raster layers. The dependency of the future state ($t + 1$) of a pixel on the set of transition rules (ϕ) and the current state of the pixel was examined as per the following equation (Kumar et al., 2009):

$$a_{i,j}^{t+1} = \phi(A_{i,j}^t) \quad (ii)$$

The transition rules (ϕ) were the function of a set of conditional statements with threshold values, represented as:

$$\phi = f(T, B) \quad (iii)$$

Eq. (iii) shows that the transition rules are a function of T, the set of threshold values for all the affecting parameters and B, a set of built-up count values in the kernel associated with every set of T.

$$T = \{T_R, T_C, T_P, T_S\} \quad (iv)$$

$$B = \{B_R, B_C, B_P, B_S\} \quad (v)$$

where, T_R , T_C , T_P , and T_S are the threshold values for proximity to roads, distance from CBD, population density and slope value respectively; B_R , B_C , B_P , and B_S are the corresponding number of built-up pixels in the test kernel for every element that belongs to T.

The rules in the CA model adopted are as per the general conditions prevailing in the real world. (a) The built-up land and water body classes were exempted from elimination, (b) the vegetation land or others class may transform into built-up land based on threshold values (T) and neighboring built-up pixel count (B) in case the test pixel falls in the non-restricted category in the restricted areas layer.

3.3. Model calibration

The model calibration was initiated using the satellite-based LULC for the year 1989 to simulate the LULC for 1994, then using the satellite-based 1994 LULC to simulate for 1999 and so on, ending by simulating the 2014 LULC using the 2009 LULC data. The model deduced the best-set threshold values that exhibit the closest possible result as per the real world (Kumar et al., 2009), statistically and spatially by simulating the LULC of time t_2 by using LULC of time t_1 and the driving parameters. This was done by trial and error, obtaining the threshold values of all the four factors (T_R , T_C , T_P , and T_S) and their associated built-up pixel count values (B_R , B_C , B_P , and B_S). In addition, the script also monitored the contribution of each affecting factor in the

generation of the new built-up pixel. Post-calibration, the threshold values were plotted and the trendlines were used to project thresholds for the future stage to predict future built-up extent.

For the sake of accuracy at each step of the simulation, the PCA (principal component analysis) was used (Ramachandra & Kumar, 2009), where the difference between two images is computed by spatially subtracting the built-up pixels of time t_2 from the corresponding pixels of time t_1 . Here, dichotomous built-up layers were extracted out of the satellite-based and simulated LULC images of the same time period. The built-up land common in both the images was eliminated by subtraction and produced non-zero (1 or -1) values in case of a mismatch. The proportion of such non-zero values with respect to the total number of built-up pixels of the satellite-based images was considered for accurate percentage computation.

4. Results and discussion

The satellite-based LULC maps were prepared and analysed to deduce the land use/land cover change and urban growth patterns in Delhi during 1989–2014. Later, the major contributing factors to urban growth were analysed to calibrate the model and to project the future extent of built-up. Model calibration was given attention to achieve best possible results.

4.1. Land use/land cover mapping and urban growth

Multi-temporal satellite data was used to map the land use/land cover at 5 year intervals for the years 1989–2014. This was termed the actual (satellite-based) LULC. It was later used to simulate LULC for the period 1994–2024 and termed the simulated LULC. These simulations were correlated with satellite-based LULC during the model calibration process (for the years 1994–2014).

4.1.1. Satellite-based land use/land cover mapping and urban growth

It was found that the actual (satellite-based) built-up land has increased from 166 km² to 623 km² during 1989–2014 with 30.3% change. The periodic observation exhibits that the built-up area was 166 km² (11% of total area) in 1989, which increased 273 km² (18%) in 1994 with 7% growth primarily in the southern and north-western regions (Fig. 3(a–j) and Table 3). In 1999, it increased to 355 km² (23.6%) with 5.6% growth primarily in northern and western regions and later increased to 426 km² (28.3%) in 2004 with 4.7% growth majorly in western regions. The built-up area increased to 520 km² (34.6%) in 2009 with 6.3% growth (primarily observed in the north-west and south-west regions), which later increased to 623 km² (41.4%) in 2014 with 6.8% growth significantly in the northern regions.

The overall change in the vegetation area since 1989 to 2014 was observed to be -2.6%. The vegetation cover occupied 206 km² in 1989, which decreased to 200 km² (1994) with -0.4% change. It later decreased to 197 km² (13.1%) in 1999 with -0.2% change and to 192 km² (12.7%) in 2004 with -0.3% change. In 2009, vegetation cover further decreased to 181 km² (12%) with -0.7% change and to 166 km² (11%) with -1% change in 2014. The overall change observed in the water features class from 1989 to 2014 was -0.4%. The area covered by water bodies was 14 km² (0.9%) in the year 1989, which decreased to 12 km² (0.8%) in 1994 with -0.1% change. In 1999, this area decreased to 8 km² (0.5%) with -0.3% change and remained constant till 2004. In 2009, the total area under water bodies increased to 11 km² (0.7%) with 0.2% change and later decreased to 7 km² (0.5%) in the year 2014 with -0.2% change. The overall decrease in the others feature class was -27.3%. All the remaining features that were put into the category others covered a total area of 1165 km² (74.3%) in the year 1989, which decreased to 1017 km² (67.7%) in 1994 with -6.6% change. In 1999, the area of others class decreased to 943 km² (62.7%) with -5% change, further decreasing to 877 km² (58.3%) in 2004 with -4.4% change. In 2009, the area under

others class was decreased to 791 km² (52.6%) with -5.7% change and later to 707 km² (47%) in 2014 with -5.6% change. The study exhibits the direct influence of rapid built-up growth on other LULC classes during 1989–2014.

In recent years, it has been observed that rapid urban growth intensifies various urban problems. The spatio-temporal LULC mapping exhibits that the built-up land was largely concentrated in the eastern and central regions of Delhi, primarily due to the presence of the Yamuna River, which provided a strong base for the development of urban settlements in the last 800 years. Later, the built-up was expanded in the west and north due to the availability of suitable sites and the diverse urban functions being performed, leading to rapid population growth. The non-built-up (viz., vegetation, water bodies) features are intrinsic components of the built-up areas as they regulate the basic man-environment dynamic in the urban milieu. Rapid transformation and the persistent spread of impervious structures fundamentally alter the natural landscape and influences habitability for urban dwellers.

The area statistics of the actual and simulated LULC during the year 1989–2014 is mentioned in Table 3. The actual LULC reports higher growth rates initially (1989–1999) and minor decreasing rates during later periods (2004–2014). A similar growth pattern is seen in the simulated LULC statistics as well, pointing towards reliable model calibration.

4.2. Urban growth modelling

Urban growth modelling was performed in order to forecast the future patterns of urban growth for the years 2019 and 2024 using an earlier LULC map and various contributing factors viz., proximity to major roads and CBD, district level population density data and slope.

4.2.1. Urban growth contributing factor

The study indicates that an erratic mixture of the influence of road, CBD, and geomorphic parameters resulted in the densification of the built-up in the cores areas and in the origination of informal settlements in the more remote pockets. The various contributing parameters are discussed in the following sections.

4.2.1.1. Land use/land cover. The likelihood of different LULC classes transforming to built-up land is different. Therefore, a higher rank was assigned to the others class, followed by vegetation, depending on the availability of built-up land in the neighboring area. Built-up land and water bodies were assumed to be a non-transforming class in the modelling.

4.2.1.2. Proximity to major roads. The road network map points to a very high road density in the central parts of the city and lower density in the north-east and south-east. The majority of the suburban region has moderate to very low road density (Fig. 4(a)). Considering the role of major roads in the urbanisation process, the areas nearer to roads were given a priority for growth due to high accessibility, and vice versa.

4.2.1.3. Proximity to central business district. The CBD acts as a major multi-urban functional zone. Proximity to roads and the CBD were taken into account in order to track non-uniform growth in any direction. Kumar et al. (2009) considered 8 different directional zones [East (E), West (W), North (N), South (S), Northeast (NE), Northwest (NW) Southeast (SE), and Southwest (SW)], to represent the directional patterns of urban growth. A robust attempt has been made in the present study to capture this directional pattern by considering proximity to roads and CBD to reduce the complexity of modelling and predicting directional growth patterns. Distance from the CBD influenced urban growth majorly in the central area, and its effect decreased as distance increased (Table 4). Thus, in the early 90s, people settled in the more remote pockets of the city probably due to the lower

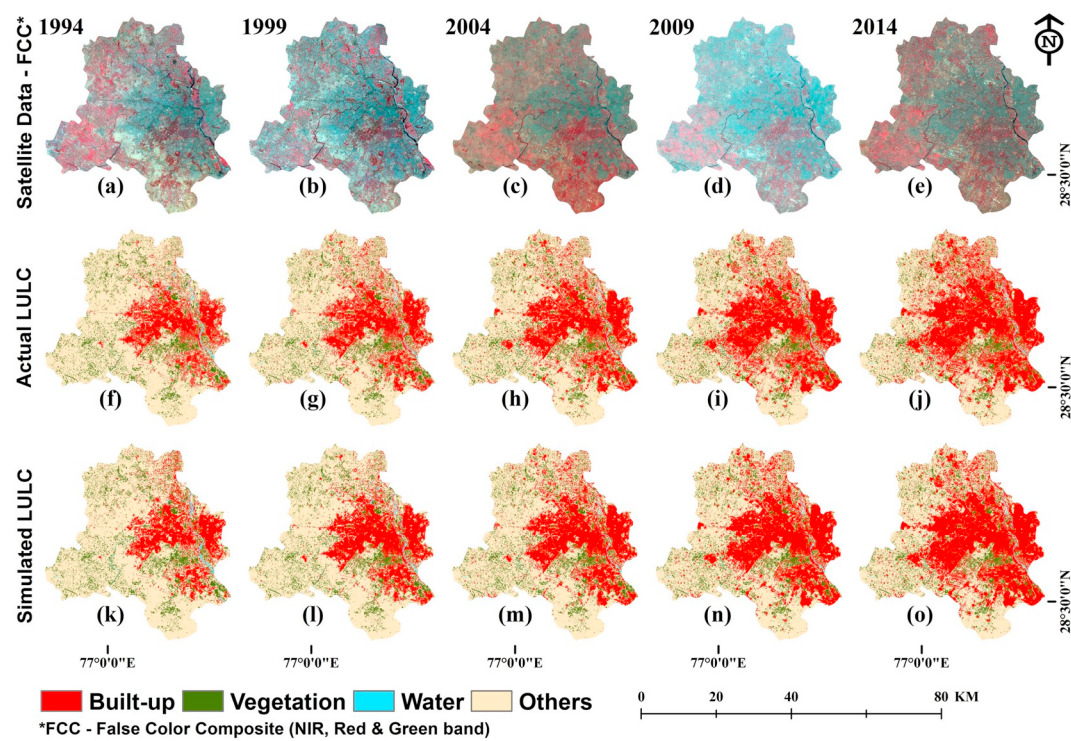


Fig. 3. LANDSAT satellite images (a to e) (obtained from USGS), satellite-based LULC maps (f to j) and simulated LULC map (k to o) of Delhi for the year 1994 (a, f, k), 1999 (b, g, l), 2004 (c, h, m), 2009 (d, i, n) and 2014 (e, j, o).

land rates. In due course, people preferred to settle in already defined neighborhoods, and this resulted in the densification of the built-up area. In contrast to this, the development of facilities in the hinterlands (Noida, Gurugram), influenced the decentralization of the urban population in the later periods.

4.2.1.4. Slope. The study indicates that relief ranges from 114 m to 261 m from mean sea level (MSL) in Delhi. The relief map indicates the slope from north to south, which is reflected by the flow of the Yamuna. Being located on the Aravalli ridge, the western parts and eastern parts have varied catchments. The relief map of Delhi exhibits a gentle slope in the north-west, and an uneven slope in the north-east and south-east (Fig. 4(c)). The majority of the area has a slope of < 3° but small portions in the east and south have slopes of up to 5°. The hillocks in the south have a steeper slope of > 5° (Fig. 4(c)). Terrain slope is a factor which exerts great control over the growth of built up. High relief and steep slopes induce higher runoff and render land less suitable for

construction, while low relief and gentle slopes provide a comparatively more stable base for buildings. This could explain why areas with a low slope were preferred for growth.

4.2.1.5. Population density. The district-level population density map of Delhi indicates a rapid increase in density in the initial stages (1991–2011) in the north-western, southern and south-western regions of the city and a moderate increase in the western region. Meanwhile, the population density in the central region (New Delhi) remained in the very high-density class of > 100,000 persons per km² (Fig. 5). A decrease in the population density was observed in the north and north-eastern regions in 1991 and 2001. This may be the result of a shift caused by a high population influx and changes in the population-related policy in Delhi.

The population density maps (2019–2024) prepared using the UN world's population projection shows an increase in the population density in the west, north, east, central and southern districts (during

Table 3

The LULC area statistics (satellite-based vs. simulated) during 1989–2014.

Type	Built-up land			Vegetation cover			Water body			Others			
	Area (km ²)	%	Δ %	Area (km ²)	%	Δ %	Area (km ²)	%	Δ %	Area (km ²)	%	Δ %	
1989	Actual	166	11.1	–	206	13.7	–	14	0.9	–	1117	74.3	–
1994	Actual	273	18.2	7.1	200	13.3	-0.4	12	0.8	-0.1	1017	67.7	-6.6
	Simulated	271	18	7	203	13.5	-0.2	14	0.9	0	1015	67.5	-6.8
1999	Actual	355	23.6	5.4	197	13.1	-0.2	8	0.6	-0.3	943	62.7	-5
	Simulated	353	23.5	5.5	195	13	-0.6	12	0.8	-0.1	942	62.7	-4.8
2004	Actual	426	28.3	4.7	192	12.8	-0.3	8	0.5	0	877	58.3	-4.4
	Simulated	430	28.6	5.1	191	12.7	-0.3	8	0.6	-0.3	873	58.1	-4.6
2009	Actual	520	34.6	6.3	181	12	-0.7	11	0.7	0.2	791	52.6	-5.7
	Simulated	519	34.5	5.9	183	12.2	-0.6	8	0.5	0	793	52.7	-5.3
2014	Actual	623	41.4	6.8	166	11.1	-1.0	7	0.5	-0.2	707	47.0	-5.6
	Simulated	614	40.8	6.3	170	11.3	-0.8	11	0.7	0.2	708	47.1	-5.7
1989–2014	Actual	–	–	30.4	–	–	-2.6	–	–	-0.4	–	–	-27.3
	Simulated	–	–	29.8	–	–	-2.4	–	–	-0.2	–	–	-27.2

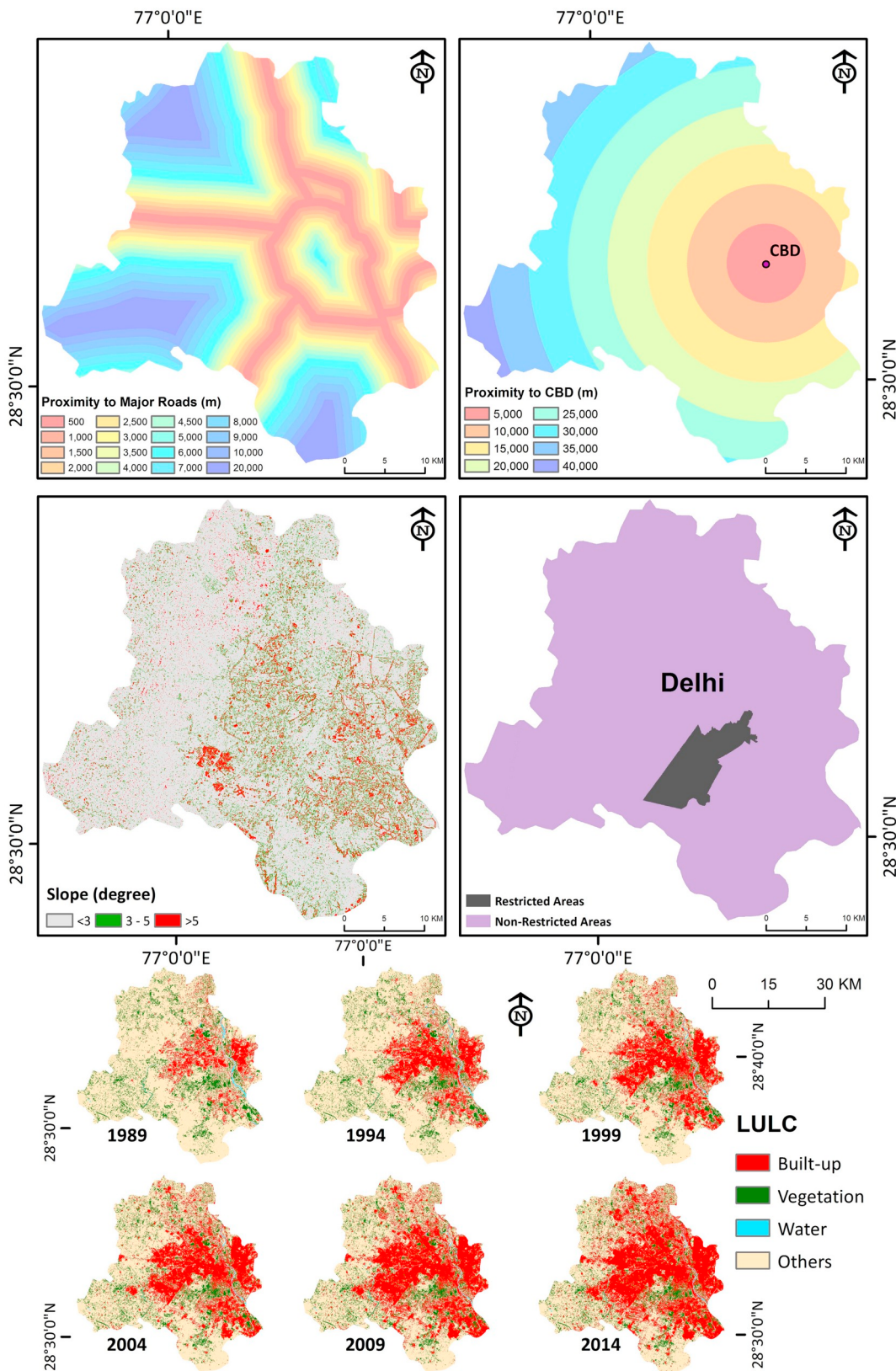


Fig. 4. Urban growth contributing factors (a) proximity to major roads, (b) proximity to Central Business District (CBD), (c) Cartosat-I DEM based slope map, (d) restricted areas, and (e) temporal satellite-based LULC classified images of 1989–2014 of Delhi region.

2011–2019), whereas the other districts did not show a change in population density. An increase in the south-western, north-eastern and eastern districts may be seen, which depicts the future expansion of

Delhi. No significant change in the population density was observed in the north-western, north, west, central and western districts during 2019–2024.

Table 4Contribution of select parameters at each stage of simulation (unit are in km²).

Parameters	1989–94 (km ²)	1994–99 (km ²)	1999–04 (km ²)	2004–09 (km ²)	2009–14 (km ²)	2014–19 (km ²)	2019–24 (km ²)
Road effect	39	29	17	33	38	46	6
Population effect	1	0	12	11	9	30	66
CBD effect	39	21	27	25	25	3	4
Slope effect	27	30	20	24	22	6	3

4.2.2. Urban growth modelling using CA

The simulated built-up for different years was analogous to the actual (satellite-based) built-up, as seen in Fig. 6. The built-up land is expected to increase from 623 km² in the year 2014 to 708 km² in 2019 (13.6% built-up growth), primarily in the western and eastern reaches of the city, and up to 787 km² in the year 2024 (11% built-up growth) with densification of the city's core area and fragmented development primarily in eastern and western parts. The vegetation cover will decrease from 166 km² in the year 2014 to 155 km² in the year 2019 (−6.6% change), and to 140 km² in the year 2024 (−9.6% change). The 'others' category features class is expected to deteriorate from 707 km² in 2014 to 633 km² in the year 2019 and finally to 569 km² in the year 2024 (Fig. 7).

4.2.3. Validation of simulated LULC

An accuracy assessment revealed a very high statistical similarity (> 98%) and high spatial similarity (> 72%) between the simulated LULC and the satellite-based LULC for the known years (1994–2014), as is given in Table 5. The spatial accuracy percentage has been computed with respect to the spatial location of the built-up land in satellite-based LULC.

The statistical accuracy check was done for the year 2014 using the satellite-based and simulated built-up extent. The computed confusion matrix exhibits an overall accuracy of 95.62% (Table 7), and the area under curve (AUC) of the receiver operating characteristic (ROC) graph (Fig. 8) was found to be as high as 0.928. The high accuracy of the

confusion matrix and AUC indicates high accuracy of the modelling. This was probably brought about due to the use of a smaller period of prediction (5 years) at regular intervals during calibration.

The transition probability matrix was computed using the temporal land use/land cover maps (Tables 7 and 8) that shows the transformation of pixels belonging to all four feature classes over a time period (1989 to 2014 and 2014 to 2024). The transition from 1989 to 2014 shows that most of the built-up land pixels remained in the same class (0.943), and a very small number of built-up pixels were transformed to water (0.001) and others classes (0.057). This can be attributed to misclassification caused by the similar reflectance of the built-up and water body (sand) class and the improved resolution of the satellite data in recent years as compared to previous. A similar issue was observed in some areas under the water class which transformed into built-up land (0.322) and the others category (0.314). The loss of vegetation (0.193) and others (0.378) class was attributed to generating new built-up land pixels.

The transition matrix during 2014 to 2024 shows that all the built-up land class pixels remain unchanged (value 1). Some of the pixels of the vegetation class transformed to built-up land (0.157), while the rest remained the same (0.843). All the water class pixels remain completely unchanged (value 1). The pixels belonging to others class contributed towards the generation of pixels of built-up land (0.195) class (Table 9). The water and others class pixels were subject to a transformation to built-up land when the conditions were satisfied as per the model. The comparison of Tables 8 and 9 also shows that the growth pattern in both

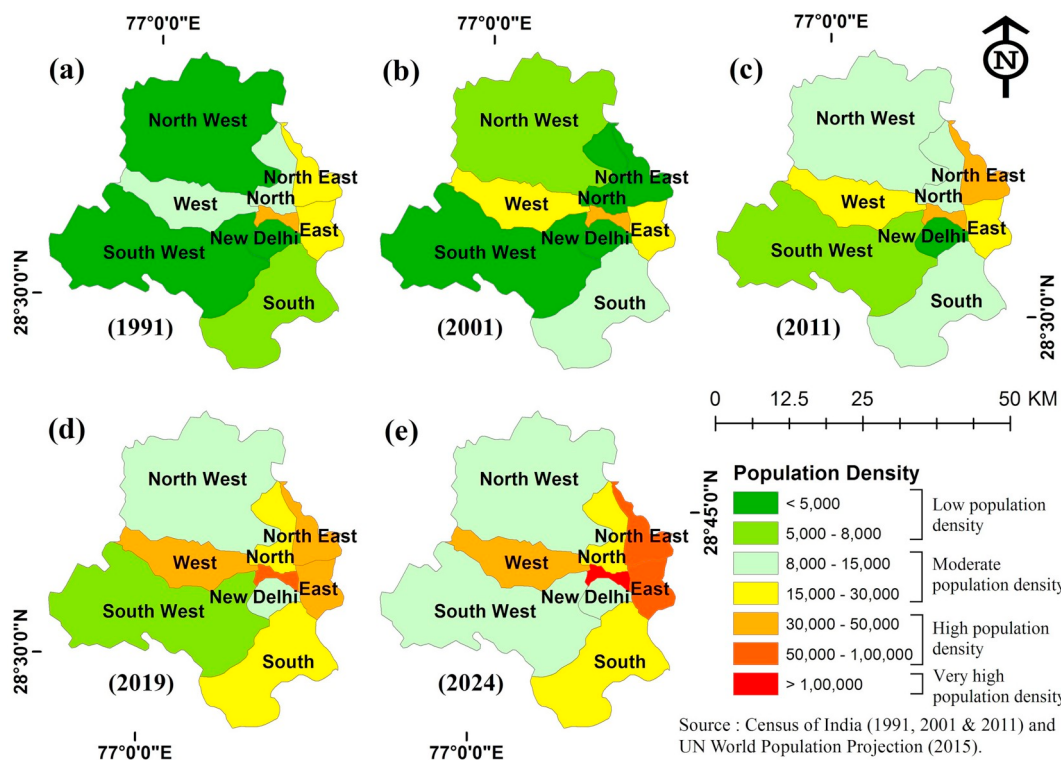


Fig. 5. Population density maps of districts in Delhi for different periods viz., (a) 1991, (b) 2001, (c) 2011, (d) 2019, and (e) 2024.

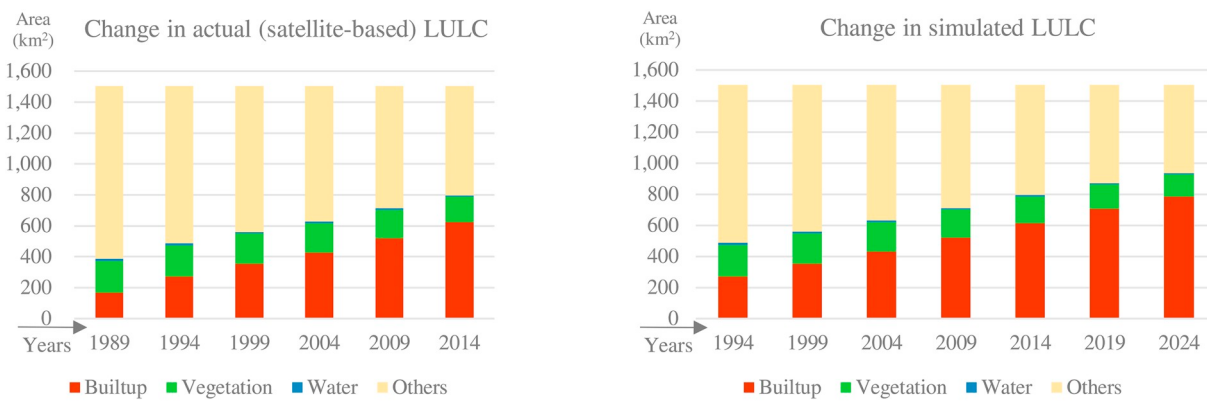


Fig. 6. Graph showing the (a) actual and, (b) simulated LULC change.

the periods is comparable considering the ground realities.

4.2.4. Influence of future urban growth on varied LULC

The built-up expansion illustrated by the CA-based urban growth model indicates a 164 km² net increase in urban area and an urban growth rate of 27.61% in the years 2014–2024 (Table 6 and Fig. 9). This will have a considerable impact on others LULC category (net loss: 138 km²) and on vegetation cover (net loss: 26 km²). The study exhibits that urban growth rates in Delhi will be higher in the period 2014–19 than in the period 2019–24. This will act as the impetus for the major loss of other LULC categories in the period 2014–19 as compared to the period 2019–24, whereas vegetation cover will witness similar impact during both the periods (Table 6).

5. Conclusion

The study encompasses spatio-temporal LULC monitoring (1989–2014) and urban growth modelling (1994–2024) of Delhi, to glean the past and future urban growth paradigm and its influence on varied land use/cover using CA model. The satellite-based and simulated LULC exhibited rapid urban growth (net increase 457 km² & 448 km²) during 1989–2014, which induced significant land use transformation in Delhi. The rapid urban growth largely altered the others class (27.3% change), followed by vegetation cover (2.6%

Table 5

The statistical variability of built-up land as per satellite-based and simulated images.

Variables	Built-up areas in km ²				
	1994	1999	2004	2009	2014
Actual (km ²)	273	355	426	520	623
Simulated (km ²)	271	353	430	519	614
Spatial accuracy	74%	88%	89%	74%	88%

change), and water body (0.4% change). The CA-based simulated LULC shows that the urban area will increase to 708 km² and 787 km² primarily in western and eastern parts during 2019 and 2014, respectively. The rapid urban growth will replace and transform the ‘others’ LULC category (net loss 138 km²) and the vegetation cover category (net loss 26 km²) during 2014–24.

The change dynamics were parallel in the simulated and satellite-based LULC over the known years (1989–2014). The spatial variation analysis conducted using the PCA technique exhibited high built-up accuracy for the years 1999 and 2014 (88%), followed by 2004 (89%), then 2009 and 1994 (72%). The overall accuracy of the confusion matrix (95.62%) and the area under ROC curve (0.928) computed using the satellite-based and simulated built-up patch for the year 2014

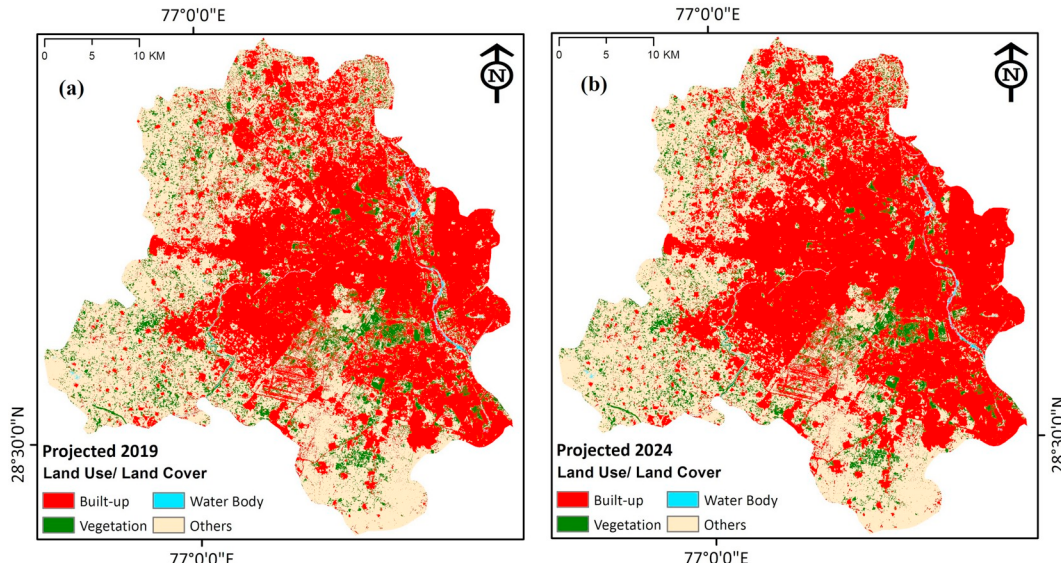


Fig. 7. CA model-based simulated built-up growth for the year (a) 2019, and (b) 2024.

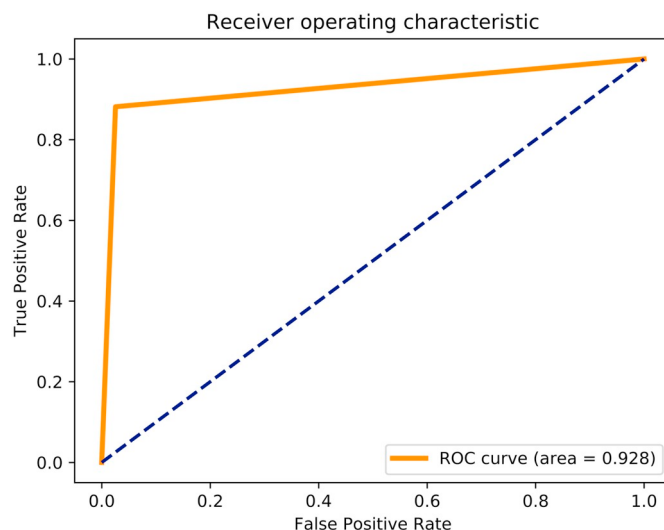


Fig. 8. Receiver operating characteristic curve for the actual and simulated built-up land during 2014.

Table 6

Area statistics of varied classes for the year 2014 and projected 2019 and 2024 with the percentage change.

	2014 (km ²)	2019 (km ²)	2024 (km ²)	% Change 2014–2024
Built-up	623	708	787	26.3
Vegetation	166	155	140	-15.3
Water	7	7	7	0
Others	707	633	569	-19.5

points to the high accuracy of the modelling. An attempt was made to determine the dependencies of contributing factors on the growth process over time (1994–24), which evidenced the high influence of proximities to built-up and CBD during the initial period of observation, whereas the contribution of population density escalated during the

Table 7
Confusion matrix for actual and simulated 2014 built-up pixels.

	Predicted		Percentage correct	Overall accuracy
	Non-built-up	Built-up		
Actual	Non-built-up	2,761,799	72,085	97.45%
	Built-up	81,921	60,975	88.15%

Table 8
Transition matrix (satellite-based 1989 to 2014).

LULC	Built-up	Vegetation	Water	Others
Built-up	0.943	0	0.001	0.057
Vegetation	0.193	0.807	0	0
Water	0.322	0	0.364	0.314
Others	0.378	0	0.002	0.620

Table 9
Transition matrix (satellite-based 2014 to 2024).

	Built-up	Vegetation	Water	Others
Built-up	1	0	0	0
Vegetation	0.157	0.843	0	0
Water	0	0	1	0
Others	0.195	0	0	0.805

later periods. A combination of these factors induced urban densification in the existing built-up area (core) and sprawl in the periphery at varied rates and arbitrary patterns.

The well-calibrated CA model was able to replicate the real-world growth process very well statistically, whereas the spatial analogy was moderate. This moderately high spatial accuracy shows the limitations in the context of Indian cities, where urban growth is primarily haphazard and unplanned. This study focused on escalating the reliability of the CA model and used the data of six evenly spaced stages of growth to calibrate the model to project urban growth for the near future.

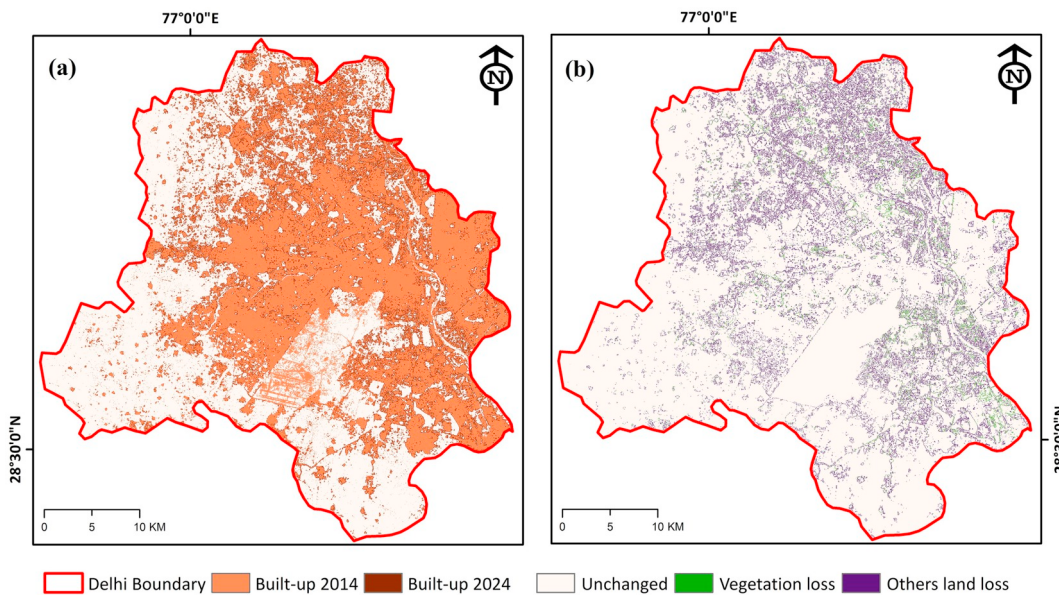


Fig. 9. Map representing (a) urban growth and (b) its influence on varied LULC during 2014–24.

Acknowledgement

The authors wish to acknowledge to United States Geological Survey (USGS) and Indian Space Research Organization (ISRO) for providing the temporal LANDSAT satellite data and Cartosat DEM (respectively) that has been used in the study. Authors are thankful to Dr. Uttam Kumar (International Institute of Information Technology, Bangalore) for his support. The authors are also grateful to Rekha Raghunathan, Indian Institute for Human Settlements (IIHS) for the valuable edits.

References

- Aljoufie, M., Zuideest, M., Brussel, M., & van Maarseveen, M. (2013). Spatial-temporal analysis of urban growth and transportation in Jeddah City, Saudi Arabia. *Cities*, 31, 57–68. <https://doi.org/10.1016/J.CITIES.2012.04.008>.
- Aljoufie, M., Zuideest, M., Brussel, M., van Vliet, J., & van Maarseveen, M. (2013). A cellular automata-based land use and transport interaction model applied to Jeddah, Saudi Arabia. *Landscape and Urban Planning*, 112, 89–99. <https://doi.org/10.1016/j.landurbplan.2013.01.003>.
- Arsanjani, J. J., Kainz, W., & Mousivand, A. J. (2011). Tracking dynamic land-use change using spatially explicit Markov Chain based on cellular automata: The case of Tehran. *International Journal of Image and Data Fusion*, 2(4), 329–345. <https://doi.org/10.1080/19479832.2011.605397>.
- Batty, M. (1997). Cellular automata and urban form: A primer. *Journal of the American Planning Association*, 63(2), 266–274. <https://doi.org/10.1080/01944369708975918>.
- Batty, M. (1998). Urban evolution on the desktop: Simulation with the use of extended cellular automata. *Environment and Planning A*, 30(11), 1943–1967. <https://doi.org/10.1068/a301943>.
- Batty, M., & Xie, Y. (1994). From cells to cities. *Environment and Planning B, Planning & Design*, 21(7), S31–S48. <https://doi.org/10.1068/b21S031>.
- Berberoğlu, S., Akin, A., & Clarke, K. C. (2016). Cellular automata modeling approaches to forecast urban growth for Adana, Turkey: A comparative approach. *Landscape and Urban Planning*, 153, 11–27. <https://doi.org/10.1016/j.landurbplan.2016.04.017>.
- Bhatta, B. (2009). Analysis of urban growth pattern using remote sensing and GIS: A case study of Kolkata, India. *International Journal of Remote Sensing*, 30(18), 4733–4746. <https://doi.org/10.1080/01431160802651967>.
- Census (2011). *Primary census abstracts, registrar general of India, ministry of home affairs, Government of India*.
- Chadchan, J., & Shankar, R. (2012). An analysis of urban growth trends in the post-economic reforms period in India. *International Journal of Sustainable Built Environment*, 1(1), 36–49. <https://doi.org/10.1016/J.IJSBE.2012.05.001>.
- Chen, Y., Li, X., Liu, X., Ai, B., & Li, S. (2016). Capturing the varying effects of driving forces over time for the simulation of urban growth by using survival analysis and cellular automata. *Landscape and Urban Planning*, 152, 59–71. <https://doi.org/10.1016/j.landurbplan.2016.03.011>.
- Clarke, K. C., & Gaydos, L. J. (1998). Loose-coupling a cellular automaton model and GIS: Long-term urban growth prediction for San Francisco and Washington/Baltimore. *International Journal of Geographical Information Science*, 12(7), 699–714. <https://doi.org/10.1080/136588198241617>.
- Clarke, K. C., Hoppen, S., & Gaydos, L. (1997). A self-modifying cellular automaton model of historical urbanization in the San Francisco Bay area. *Environment and Planning B, Planning & Design*, 24(2), 247–261. <https://doi.org/10.1068/b240247>.
- Deep, S., & Saklani, A. (2014). Urban sprawl modeling using cellular automata. *The Egyptian Journal of Remote Sensing and Space Science*, 17(2), 179–187. <https://doi.org/10.1016/j.ejrs.2014.07.001>.
- Diksha, & Kumar, A. (2017). Analysing urban sprawl and land consumption patterns in major capital cities in the Himalayan region using geoinformatics. *Applied Geography*, 89, 112–123. <https://doi.org/10.1016/J.APGEOG.2017.10.010>.
- Dubovyk, O., Sliuzas, R., & Flacke, J. (2011). Spatio-temporal modelling of informal settlement development in Sancaktepe district, Istanbul, Turkey. *ISPRS Journal of Photogrammetry and Remote Sensing*, 66(2), 235–246. <https://doi.org/10.1016/j.isprsjprs.2010.10.002>.
- Feng, Y., Liu, Y., Tong, X., Liu, M., & Deng, S. (2011). Modeling dynamic urban growth using cellular automata and particle swarm optimization rules. *Landscape and Urban Planning*, 102(3), 188–196. <https://doi.org/10.1016/j.landurbplan.2011.04.004>.
- Global Cities 2030 (2016). Retrieved from <https://www.oxfordeconomics.com/publication/download/270006>.
- Guttikunda, S. K., & Calori, G. (2013). A GIS based emissions inventory at 1 km × 1 km spatial resolution for air pollution analysis in Delhi, India. *Atmospheric Environment*, 67, 101–111. <https://doi.org/10.1016/J.ATMOSENV.2012.10.040>.
- Han, J., Hayashi, Y., Cao, X., & Imura, H. (2009). Application of an integrated system dynamics and cellular automata model for urban growth assessment: A case study of Shanghai, China. *Landscape and Urban Planning*, 91(3), 133–141. <https://doi.org/10.1016/j.landurbplan.2008.12.002>.
- Hu, Z., & Lo, C. P. (2007). Modeling urban growth in Atlanta using logistic regression. *Computers, Environment and Urban Systems*, 31(6), 667–688. <https://doi.org/10.1016/j.compenvurbsys.2006.11.001>.
- Jain, M., Dimri, A. P., Niyogi, D., Jain, M., Dimri, A. P., & Niyogi, D. (2016). Urban sprawl patterns and processes in Delhi from 1977 to 2014 based on remote sensing and spatial metrics approaches. *Earth Interactions*, 20(14), 1–29. <https://doi.org/10.1175>.
- Jat, M. K., Choudhary, M., & Saxena, A. (2017). Application of geo-spatial techniques and cellular automata for modelling urban growth of a heterogeneous urban fringe. *The Egyptian Journal of Remote Sensing and Space Science*, 20(2), 223–241. <https://doi.org/10.1016/J.EJRS.2017.02.002>.
- Jokar Arsanjani, J., Helbich, M., Kainz, W., & Darvishi Boloorani, A. (2013). Integration of logistic regression, Markov chain and cellular automata models to simulate urban expansion. *International Journal of Applied Earth Observation and Geoinformation*, 21, 265–275. <https://doi.org/10.1016/J.JAG.2011.12.014>.
- Kumar, A. (2016). Urban footprints on environment: A geoinformatics approach. In M. Gaur, C. B. Pandey, & R. K. Goyal (Eds.). *Remote sensing for natural resources monitoring & management* (pp. 339–348). Jodhpur: Scientific Publishers.
- Kumar, A., & Pandey, A. C. (2016). Geoinformatics based groundwater potential assessment in hard rock terrain of Ranchi urban environment, Jharkhand state (India) using MCDM-AHP techniques. *Groundwater for Sustainable Development*, 2–3, 27–41. <https://doi.org/10.1016/J.GSD.2016.05.001>.
- Kumar, A., & Pandey, A. C. (2017). Analyzing seismic activities during 1900 to 2015 to assess urban risk in Nepal Himalayas using Geoinformatics. *Journal of Urban and Environmental Engineering*, 11(2), 133–141. <https://doi.org/10.4090/juee.2015.v11n3.133-141>.
- Kumar, U., Mukhopadhyay, C., & Ramachandra, T. V. (2009). Cellular automata and Genetic Algorithms based urban growth visualization for appropriate land use policies. In *Fourth annual international conference on public policy and management* Bangalore, India: Centre for Public Policy, Indian Institute of Management (IIMB). Retrieved from http://wgbis.ces.iisc.ernet.in/energy/paper/iimb_cellular_automata/index.htm.
- Lal, K., Kumar, D., & Kumar, A. (2017). Spatio-temporal landscape modeling of urban growth patterns in Dhanbad Urban Agglomeration, India using geoinformatics techniques. *The Egyptian Journal of Remote Sensing and Space Science*, 20(1), 91–102. <https://doi.org/10.1016/J.EJRS.2017.01.003>.
- Li, G. Y., Chen, S. S., Yan, Y., & Yu, C. (2015). Effects of urbanization on vegetation degradation in the Yangtze River Delta of China: Assessment based on SPOT-VGT NDVI. *Journal of Urban Planning and Development*, 141(4), 05014026. [https://doi.org/10.1061/\(ASCE\)UP.1943-5444.0000249](https://doi.org/10.1061/(ASCE)UP.1943-5444.0000249).
- Ligtenberg, A., Bregt, A. K., & van Lammeren, R. (2001). Multi-actor-based land use modelling: Spatial planning using agents. *Landscape and Urban Planning*, 56(1–2), 21–33. [https://doi.org/10.1016/S0169-2046\(01\)00162-1](https://doi.org/10.1016/S0169-2046(01)00162-1).
- Lo, C. P., & Yang, X. (n.d.). Drivers of land-use/land-cover changes and dynamic modeling for the Atlanta, Georgia Metropolitan Area. Retrieved from https://www.asprs.org/wp-content/uploads/pers/2002journal/october/2002_oct_1073-1082.pdf
- Maiti, S., & Agrawal, P. K. (2005). Environmental degradation in the context of growing urbanization: A focus on the metropolitan cities of India. *Journal of Human Ecology*, 17(4), 277–287. <https://doi.org/10.1080/09709274.2005.11905793>.
- McMichael, A. J. (2000). The urban environment and health in a world of increasing globalization: Issues for developing countries. *Bulletin of the World Health Organization*, 78(9), 1117–1126. Retrieved from <http://www.ncbi.nlm.nih.gov/pubmed/11019460>.
- Mitsova, D., Shuster, W., & Wang, X. (2011). A cellular automata model of land cover change to integrate urban growth with open space conservation. *Landscape and Urban Planning*, 99(2), 141–153. <https://doi.org/10.1016/J.LANDURBPLAN.2010.10.001>.
- Mohan, M., Pathan, S. K., Narendrareddy, K., Kandya, A., & Pandey, S. (2011). Dynamics of urbanization and its impact on land-use/land-cover: A case study of megacity Delhi. *Journal of Environmental Protection*, 02(09), 1274–1283. <https://doi.org/10.4236/jep.2011.29147>.
- Mondal, M. S., Sharma, N., Garg, P. K., & Kappas, M. (2016). Statistical independence test and validation of CA Markov land use land cover (LULC) prediction results. *The Egyptian Journal of Remote Sensing and Space Science*, 19(2), 259–272. <https://doi.org/10.1016/J.EJRS.2016.08.001>.
- Munshi, T., Zuideest, M., Brussel, M., & van Maarseveen, M. (2014). Logistic regression and cellular automata-based modelling of retail, commercial and residential development in the city of Ahmedabad, India. *Cities*, 39, 68–86. <https://doi.org/10.1016/j.jcites.2014.02.007>.
- Mustafa, A., Cools, M., Saadi, I., & Teller, J. (2017). Coupling agent-based, cellular automata and logistic regression into a hybrid urban expansion model (HUEM). *Land Use Policy*, 69, 529–540. <https://doi.org/10.1016/J.LANDUSEPOL.2017.10.009>.
- Mustafa, A., Heppenstall, A., Omrani, H., Saadi, I., Cools, M., & Teller, J. (2018). Modelling built-up expansion and densification with multinomial logistic regression, cellular automata and genetic algorithm. *Computers, Environment and Urban Systems*, 67, 147–156. <https://doi.org/10.1016/J.COMPENVURBSYS.2017.09.009>.
- Nagar, P. K., Singh, D., Sharma, M., Kumar, A., Aneja, V. P., George, M. P., ... Shukla, S. P. (2017). Characterization of PM2.5 in Delhi: Role and impact of secondary aerosol, burning of biomass, and municipal solid waste and crustal matter. *Environmental Science and Pollution Research*, 24(32), 25179–25189. <https://doi.org/10.1007/s11356-017-0171-3>.
- Nong, Y., & Du, Q. (2011). Urban growth pattern modeling using logistic regression. *Geospatial Information Science*, 14(1), 62–67. <https://doi.org/10.1007/s11806-011-0427-x>.
- Peng, X., Chen, X., & Cheng, Y. (1997). Urbanization and its consequences - a generalized model for cellular urban dynamics. *Demography*, 2(28), 350–373. Retrieved from <https://www.eolss.net/sample-chapters/C04/E6-147-18.pdf>.
- Rafiee, R., Mahiny, A. S., Khorasani, N., Darvishsefat, A. A., & Danekar, A. (2009). Simulating urban growth in Mashhad City, Iran through the SLEUTH model (UGM). *Cities*, 26(1), 19–26. <https://doi.org/10.1016/j.cities.2008.11.005>.
- Ramachandra, T. V., Bharath Aithal, H., Vinay, S., Joshi, N. V., Kumar, U., & Rao, K. V. (2013). Modelling urban revolution in greater Bangalore, India. *30th annual in-house symposium on space science and technology* Bangalore, India: ISRO-IIIS Space

- Technology Cell, Indian Institute of Science. Retrieved from http://wgbis.ces.iisc.ernet.in/energy/water/paper/isrostc_urban_revolution/index.htm.
- Ramachandra, T. V., & Kumar, U. (2009). Land surface temperature with land cover dynamics: Multi-resolution, spatio-temporal data analysis of greater Bangalore. *International Journal of Geoinformatics*, 5(3), Retrieved from <http://creativecity.gssc.osaka-cu.ac.jp/IJG/article/view/480>.
- Ramachandraiah, C., & Prasad, S. (2004). *Impact of urban growth on water bodies The case of hyderabad*. Centre For Economic And Social Studies. Retrieved from <http://www.cess.ac.in/cesshome/wp/wp-60.pdf>.
- Sahu, N., Deori, M., & Ghosh, I. (2018). Metagenomics study of contaminated sediments from the Yamuna River at Kalindi Kunj, Delhi, India. *Genome Announcements*, 6(1), <https://doi.org/10.1128/genomeA.01379-17> e01379-17.
- Santé, I., Garcia, A. M., Miranda, D., & Crecente, R. (2010). Cellular automata models for the simulation of real-world urban processes: A review and analysis. *Landscape and Urban Planning*, 96(2), 108–122. <https://doi.org/10.1016/j.landurbplan.2010.03.001>.
- Shafizadeh Moghadam, H., & Helbich, M. (2013). Spatiotemporal urbanization processes in the megacity of Mumbai, India: A Markov chains-cellular automata urban growth model. *Applied Geography*, 40, 140–149. <https://doi.org/10.1016/J.APGEOG.2013.01.009>.
- Sharma, A. K., Baliyan, P., & Kumar, P. (2018). Air pollution and public health: The challenges for Delhi, India. *Reviews on Environmental Health*, 33(1), 77–86. <https://doi.org/10.1515/reveh-2017-0032>.
- Shi, W., & Pang, M. Y. C. (2000). Development of Voronoi-based cellular automata -an integrated dynamic model for geographical information systems. *International Journal of Geographical Information Science*, 14(5), 455–474. <https://doi.org/10.1080/13658810050057597>.
- Siddiqui, A., Siddiqui, A., Maithani, S., Jha, A. K., Kumar, P., & Srivastav, S. K. (2017). Urban growth dynamics of an Indian metropolitan using CA Markov and logistic regression. *The Egyptian Journal of Remote Sensing and Space Science*. <https://doi.org/10.1016/j.ejrs.2017.11.006>.
- Statistical Abstract of Delhi. Retrieved from <http://www.indiaenvironmentportal.org.in/files/file/Stattistical%20Abstract%20of%20Delhi%202014.pdf>.
- Thapa, R. B., & Murayama, Y. (2010). Drivers of urban growth in the Kathmandu valley, Nepal: Examining the efficacy of the analytic hierarchy process. *Applied Geography*, 30(1), 70–83. <https://doi.org/10.1016/J.APGEOG.2009.10.002>.
- Thapa, R. B., & Murayama, Y. (2012). Scenario based urban growth allocation in Kathmandu Valley, Nepal. *Landscape and Urban Planning*, 105(1–2), 140–148. <https://doi.org/10.1016/J.LANDURBPLAN.2011.12.007>.
- Torrens, P. M., & O'Sullivan, D. (2001). Cellular automata and urban simulation: Where do we go from here? *Environment and Planning B, Planning & Design*, 28(2), 163–168. <https://doi.org/10.1068/b2802ed>.
- United Nation Population Projection 2030*.
- Vaz, E., De Noronha, T., & Nijkamp, P. (2014). Exploratory landscape metrics for agricultural sustainability. *Agroecology and Sustainable Food Systems*, 38(1), 92–108. <https://doi.org/10.1080/21683565.2013.825829>.
- Waldrop, M. M. (1992). *Complexity: The emerging science at the edge of order and chaos*. New York: Simon & Schuster. Retrieved from <https://uberty.org/wp-content/uploads/2017/04/Waldrop-M.-Mitchell-Complexity-The-Emerging-Science-at-Edge-of-Order-and-Chaos.pdf>.
- Wu, F., & Webster, C. J. (2000). Simulating artificial cities in a GIS environment: Urban growth under alternative regulation regimes. *International Journal of Geographical Information Science*, 14(7), 625–648. <https://doi.org/10.1080/136588100424945>.
- Zhao, Y., Zhao, J., & Murayama, Y. (2008). In L. Liu, X. Li, K. Liu, X. Zhang, & A. Chen (Eds.). *Modeling and predicting urban growth pattern of the Tokyo metropolitan area based on cellular automata* (pp. 71431Q). . <https://doi.org/10.11117/12.812591>.